IL NUOVO CIMENTO **47 C** (2024) 236
DOI 10.1393/ncc/i2024-24236-3

COLLOQUIA: HADRON2023

Recent measurements and prospects from analysis of fixed-target collisions at LHCb

L. L. PAPPALARDO(*)
Dipartimento di Fisica e Scienze della Terra, Università di Ferrara - Ferrara, Italy

received 21 December 2023

Summary. — The LHCb spectrometer has the unique capability to function as a fixed-target experiment by injecting gas into the LHC beampipe while proton or ion beams are circulating. The resulting beam-gas collisions cover an unexplored energy range that is above previous fixed-target experiments, but below the RHIC or LHC collider energies. Here we present recent results on J/ψ and D^0 production from pNe and PbNe fixed-target collisions at LHCb. Some preliminary results obtained during the commissioning of the upgraded system SMOG2 are also reported.

1. – Introduction

The LHCb experiment [1, 2] is based on a single-arm forward spectrometer covering the pseudorapidity range $2 < \eta < 5$. It was designed for the study of hadrons containing b or c quarks and has excellent vertexing, tracking and particle identification capabilities. Furthermore, LHCb provides the unique opportunity at the LHC to operate in a fixed-target mode, thanks to the System for Measuring Overlap with Gas (SMOG). This system, originally designed for precise luminosity measurements [3], allows to inject noble gas (helium, neon and argon) inside the primary LHC vacuum around the LHCb vertex detector (VELO). Since 2015 LHCb has started to exploit SMOG to perform physics measurements, using special fills not devoted to pp physics, and exploiting both p and Pb LHC beams. This allows to perform a variety of studies of great interest ranging from nucleon structure to heavy-ion physics as well as cosmic rays physics and dark matter search. Recent LHCb fixed-target results in the sector of charm physics are reported in this paper, along with a brief description of the upgraded SMOG2 setup, installed during the LHC Long Shutdown 2 and in operation during the Run 3.

The LHCb Collaboration has recently reported measurements of J/ψ and D^0 production in fixed-target pNe [4, 5] and PbNe [6] collisions. Production of heavy quarks

(*) On behalf of the LHCb Collaboration.

in nucleus-nucleus interactions is a relevant probe of the transition between ordinary hadronic matter and the Quark-Gluon Plasma (QGP), in the high-density and high-temperature regime of QCD. Furthermore, several initial- and final-state effects occurring in proton-nucleus collisions can modify charmonium production with respect to proton-proton collisions. These effects include nuclear absorption, multiple scattering, and radiative energy loss. These so-called cold nuclear-matter effects depend on the collision energy, the transverse momentum and rapidity of the produced charmed mesons, as well as the size of the target nucleus. Moreover, the understanding of charmonium production and hadronization mechanisms can be significantly improved by comparison with measurements of the overall charm quark production, mainly represented by D^0 mesons. It is therefore essential to carry out charmonium and open-charm measurements over a wide range of experimental conditions.

2. – Charm production in pNe collisions at $\sqrt{s_{NN}} = 68.5\,\text{GeV}$

The production of D^0 and J/ψ mesons is studied in collisions of 2.5 TeV protons incident on neon nuclei at rest, resulting in a centre-of-mass energy per nucleon of $\sqrt{s_{NN}} = 68.5\,\text{GeV}$ [4, 5]. The integrated luminosity is determined to be $21.7 \pm 1.4\,\text{nb}^{-1}$ from the yield of electrons elastically scattering off the target Ne atoms. The measurements are performed in the ranges of transverse momentum $p_T < 8\,\text{GeV}/c$ and rapidity $2.0 < y < 4.29$ of the J/ψ and D^0 mesons. Due to the boost induced by the high-energy proton beam, the LHCb aceptance covers the negative centre-of-mass rapidity range $-2.29 < y^* < 0$. The J/ψ and D^0 candidates are reconstructed from the $\mu^+\mu^-$ and $K^-\pi^+$ decay modes, respectively, and the signal yields are obtained with extended maximum-likelihood fits to the corresponding invariant-mass distributions after all selection criteria are applied.

Figure 1 shows the D^0 and J/ψ differential production cross-sections as a function of y^* and p_T. The results are compared with several model predictions. Most features of the D^0 measurements are well described by the Vogt predictions with (Vogt 1%IC) or without (Vogt no IC) intrinsic charm contributions, both taking into account the shadowing effect [7], and by predictions (MS) including 1% intrinsic charm and 10% recombination contributions [8]. Other model predictions fail to reproduce the low or high p_T regions. Similarly, the J/ψ results are well described by predictions (Vogt) using calculations in the Color Evaporation Model carried out at Next-to-Leading Order (NLO) in the heavy-flavour cross-section, with or without a 1% intrinsic charm (IC) contribution [7]. HELAC-Onia (HO) predictions using different sets of parton distribution functions (pdfs) [9-12], underestimate the measured total cross-section. The J/ψ and D^0 productions are compared in fig. 2, where the ratio of the two cross-sections, measured in the same kinematical conditions, is reported as a function of y^* and p_T. While this ratio shows a strong dependence on p_T, no significant rapidity dependence is observed.

3. – Charm production in PbNe collisions at $\sqrt{s_{NN}} = 68.5\,\text{GeV}$

The J/ψ and D^0 production is also measured in fixed-target PbNe collisions [6], at the same centre-of-mass energy per nucleon as in the pNe measurements discussed above. The offline selection of J/ψ and D^0 candidates is similar to that of the pNe measurement. Also in this case the J/ψ and D^0 candidates are reconstructed via their

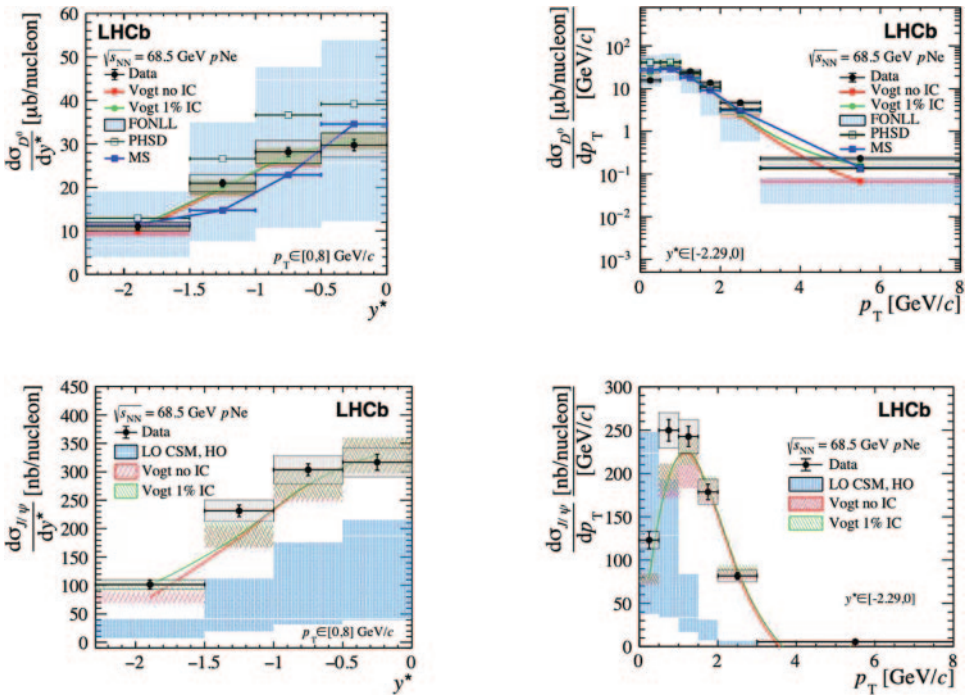

Fig. 1. – Differential production cross-sections of D^0 (upper) and J/ψ (lower) as a function of y^* (left) and p_T (right) in pNe collisions. Several model predictions are also shown.

$\mu^+\mu^-$ and $K^-\pi^+$ decays, respectively, and their signal yields are extracted from extended unbinned maximum-likelihood fits to their mass distributions. The J/ψ to D^0 cross-section ratio is shown in fig. 3 as a function of y^* and p_T. The ratio depends strongly on p_T while essentially no dependence on centre-of-mass rapidity is observed. Figure 4 shows the $J/\psi/D^0$ cross-section ratio, measured both in PbNe and in pNe collisions, as a function of the number of binary collisions, N_{coll}. While the pNe data are integrated over the impact parameter of the collisions, the PbNe data sample is divided into intervals of

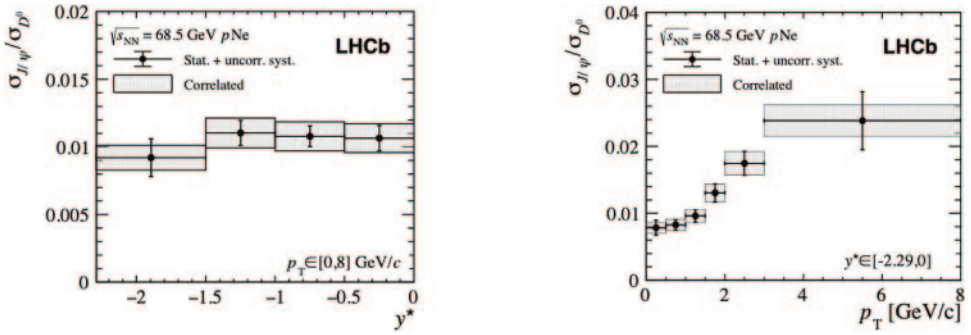

Fig. 2. – J/ψ to D^0 production cross-sections ratios in pNe collisions as a function of y^* (left) and p_T (right).

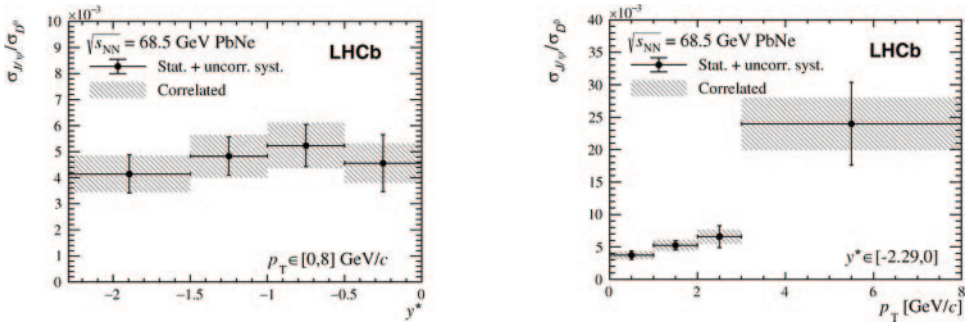

Fig. 3. – J/ψ to D^0 production cross-section ratios in PbNe collisions as a function of y^* (left) and p_T (right).

N_{coll} corresponding to different centrality intervals related to the overlap region between the two colliding nuclei.

Since small overlap regions correspond to small N_{coll} values, any suppression related to the formation of a deconfined medium should occur at large N_{coll} values. The cross-section ratio is expected to scale as $\langle N_{coll} \rangle^{\alpha'-1}$, where the parameter $\alpha' = 0.76 \pm 0.05$ is extracted from a fit to data. This value is consistent with the J/ψ production being affected by additional nuclear effects compared to D^0. However, within uncertainties, no difference in the J/ψ suppression trend is observed when comparing the PbNe largest N_{coll} bin with the pNe and PbNe smaller N_{coll} bins, indicating no evidence of an anomalous suppression that could be interpreted in terms of QGP formation.

4. – SMOG2 upgrade and commissioning

During the LHC Long Shutdown 2, the SMOG system has been upgraded. The main features of the upgraded system, called SMOG2, are the use of a storage cell for the target gas, which allows to increase the gas density by a large factor compared to SMOG, and a new and more sophysticated gas feed system, which allows for precise density measurements as well as the possibility to inject more gas species, including

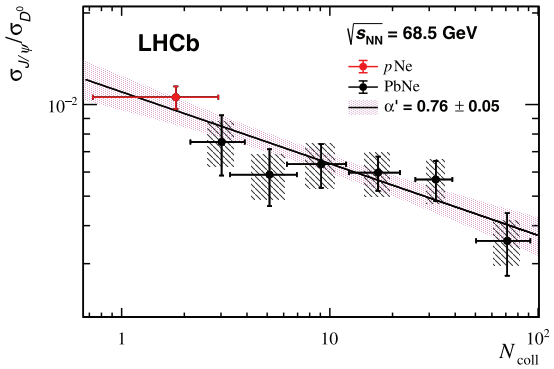

Fig. 4. – J/ψ to D^0 cross-section ratio as a function of N_{coll}. The red and black points correspond to pNe and PbNe collisions, respectively.

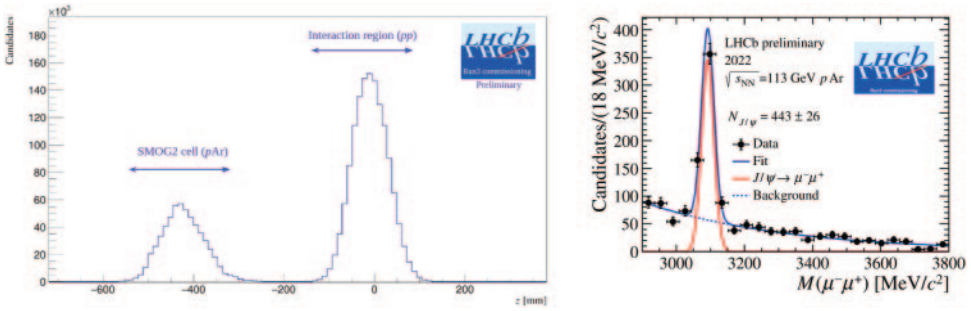

Fig. 5. – Left: distributions of pp and pAr primary vertices along the beam direction acquired during a simultaneous collider and fixed-target data taking. Right: mass distribution of J/ψ candidates collected in pAr collisions with the SMOG2 system during the commissioning phase.

hydrogen and deuterium. The SMOG2 system has been commissioned using the early Run 3 LHC beams in 2022, showing performance compatible with the expectations based on MC simulations. In particular, thanks to the well-separated beam-beam and beam-gas interaction regions achievable with the use of the storage cell, simultaneous collider and fixed-target data taking is possible, as shown in fig. 5, where the pp and pAr primary vertex regions along the beam direction appear very well separated. Figure 5 also shows the J/ψ mass distribution obtained during the SMOG2 commissioning in just 18 minutes of data taking with pAr collisions at $\sqrt{s_{NN}} = 113\,\text{GeV}$.

5. – Conclusions

The recent J/ψ and D^0 production measurements performed at LHCb in fixed-target pNe and PbNe collisions with the SMOG system have been reported. The results are consistent with the J/ψ production being affected by stronger nuclear effects compared to D^0. However, no evidence of anomalous suppression that could indicate QGP formation is reported. Starting from the Run 3 of LHC, the LHCb fixed-target physics program will be singnificantly enhanced thanks to the upgraded SMOG2 system which, among other advantages, allows a simultaneous data taking with the collider mode, a unique opportunity at the LHC.

REFERENCES

[1] LHCb Collaboration (Alves A. A. jr. *et al.*), *JINST*, **3** (2008) S08005.
[2] LHCb Collaboration (Aaij R. *et al.*), *Int. J. Mod. Phys. A*, **30** (2015) 1530022.
[3] LHCb Collaboration (Aaij R. *et al.*), *JINST*, **9** (2014) P12005.
[4] LHCb Collaboration (Aaij R. *et al.*), *Eur. Phys. J. C*, **83** (2023) 541.
[5] LHCb Collaboration (Aaij R. *et al.*), *Eur. Phys. J. C*, **83** (2023) 625.
[6] LHCb Collaboration (Aaij R. *et al.*), *Eur. Phys. J. C*, **83** (2023) 658.
[7] Vogt R., *Phys. Rev. C*, **103** (2021) 035204.
[8] Maciula R. and Szczurek A., *Phys. Lett. B*, **835** (2022) 137530.
[9] Lansberg J.-P. and Shao H.-S, *Eur. Phys. J. C*, **77** (2017) 1.
[10] Shao H.-S, *Comput. Phys. Commun.*, **198** (2016) 238.
[11] Shao H.-S, *Comput. Phys. Commun.*, **184** (2013) 2562.
[12] Kovarik *et al.*, *Phys. Rev. D*, **93** (2016) 085037.